Published by
NIGERIAN SOCIETY OF PHYSICAL SCIENCES
Available online @ https://journal.nsps.org.ng/index.php/jnsps

J. Nig. Soc. Phys. Sci. 5 (2023) 1028

Journal of the Nigerian Society of Physical Sciences

# Evaluation of ANFIS Predictive Ability Using Computed Sediment from Gullies and Dam

Stephen Olushola Oladosu[a,*], Alfred Sunday Alademomi[b,c], James Bolarinwa Olaleye[b], Joseph Olalekan Olusina[b], Tosin Julius Salami[b]

[a] *Department of Geomatics, Faculty of Environmental Sciences, University of Benin, P.M.B. 1154, Edo State, Nigeria*
[b] *Department of Surveying and Geoinformatics, Faculty of Engineering, University of Lagos, P.M.B. 12003, Akoka, Lagos State, Nigeria*
[c] *Centre for Multidisciplinary Research and Innovation, Suite C59, New Bannex Plaza, Wuze 2, Abuja, Nigeria*

## Abstract

The study proposed an Adaptive Neuro-Fuzzy Inference Systems (ANFIS) model capable of predicting sediment deposited in a dam and sediment loss-in-transit (SLIT) using the potential of a formulated mathematical relation. The input parameters consist of five members viz: the rainfall, the slope, the particle size, the velocity, and the computed total volume of sediment exited from two prominent gullies for 2017, 2018, and 2019. The outputs are the total volume of sediment deposited at the adjoining Ikpoba dam for 2017, 2018, and 2019, respectively. The Ordinary Least Square (OLS) regression model on sediment volume retained all covariates with $p<0.05$, explaining 93.8% of the variability in the dataset. The multicollinearity effect on the dataset was assessed using the Variance Inflation Factor (VIF) which was found not to pose a problem for ($VIF<5$). The model was validated using the (MSE), the (MAE), and the correlation coefficient (r). The best prediction was obtained as: ($RMSE = 0.0423$; $R^2 = 0.947$). The predicted volume of sediment was $842,895.8547 m^3$ with an error of -0.3295344% and the predicted volume of SLIT was $57,787.98 m^3$ which is an indication that ANFIS performs satisfactorily in predicting sediment volume for the gullies and the dam respectively.

DOI:10.46481/jnsps.2023.1028

*Keywords:* ANFIS, Gully Erosion, Ikpoba Dam, Sedimentation

*Article History :*
Received: 23 September 2022
Received in revised form: 21 October 2022
Accepted for publication: 21 October 2022
Published: 21 May 2023


Communicated by: O. J. Abimbola

## 1. Introduction

There are different ways in which artificial neural networks (ANN) and adaptive neuro-fuzzy inference systems (ANFIS) find application in solving real-life problems that are subject to interpretation using differential or partial differential equations numerically [1]. Water resource is one key area where soft computing, or machine learning and techniques have become indispensable for the modelling of complex, non-linear, and dynamic processes in a hydrological system domain [2]. However, their applications are found in other areas [3- 4]. The aspect of the application of soft computing methodologies in sediment study and water resources in Nigeria is quite scanty in literature [5].

Gully erosion, one of the major contributor to channel sediment is more profound in the southern part of Nigeria and is known to have contributed sizable amount of sediment as in-

*Corresponding author tel. no:
*Email address:* olushola.oladosu@uniben.edu (Stephen Olushola Oladosu)

take into dams such as the one under investigation in this work. Notable studies have been conducted in the region in various capacities on gully initiation, development, and remediation in the past as obtained in [6-11]. In 2013, the Nigerian government established the Nigeria Erosion and Watershed Management Project (NEWMAP) to oversee how best to mitigate soil erosion (particularly gully erosion) and land degradation in specific watersheds by inclusive approach [12-13]. Most often, actions to salvage the havoc pose by such environmental problem are delayed due to bureaucracy in governance. Approximately 6% of Nigeria's total landmass, relied upon by many other sectors of the economy, has either been badly damaged or degraded by gullying activities [13]. The 2% per annum growth in the population as noted by [13] is an indication that more demand will be on land use; hence, more efforts are required in addressing the issue of land degradation and gullying in the country.

Gully erosion is a process by which soil's cohesive forces are drastically weakened at particular thresholds by the action of an active run-off leading to the commencement of mass movement and the eventual creation of deep channels with a substantial amount of sediment deposited downslope [14-15]. The development of gullies causes a substantial amount of soil loss, especially in badland where sediment from gullies finds its way into the river channel and is later transported as bedload into a dam. The negative impact, in the long run, is the speedy rate of siltation and a drastic reduction in the useful life of a reservoir which when occurring will require serious attention. Gully erosion has wreaked havoc globally and has been a threat to a free, safe, and life-sustaining environment [16-20]. The motivating variables and drivers of gully initiation and development in distinct catchments are present in previous works [21-22]. On a global scale, as reported by [15], [22-23], gully erosion caused between 10 to 94 percent of soil loss, most of which finds its way downstream into a reservoir. Sediment modeling using soft computing methodologies, such as ANN, Wavelet, GA, ANFIS, C-ANFIS, and others, is described in the literature. A researcher's objective is to ascertain whether combining or complementing any models will produce an improved outcome.

According to [24-26], ANN in a broad sense, encompasses a wide range of network designs and configurations. The most common ANN in literature is the multilayer feedforward neural network (MLFFNN), which adopts a form of an interconnected perceptron that makes data and calculations flow ultimately in one direction, starting from the input data to the outputs. The most common attributes of an MLFFNN consist of an input layer, a single or multiple hidden layers, and an output layer [27-28]. During ANFIS internal training of the ANN network, the inputs of the first layer multiply an initial random weight coefficient. This development prompts the network to progress to the neurons in subsequent layers. The resulting sum is then forwarded to an activation function, which processes and transforms it to the required output. The network error of the predicted output and target output is calculated and again sent from the last layer to the previous one, thereby updating the weight coefficients. This process is called "error-back-propagation" [28- 29].

In the history of the ANFIS soft computing technique, [24-25] were pioneers. Because of its ability to deal with nonlinear phenomena, it is preferred for simulating and modelling complex hydrological systems [29-32]. Applications of ANFIS in diverse fields are quite numerous in the literature. [33], applied an ANFIS-based approach for the prediction of sediment transport in clean sewers and affirmed a satisfactory result with ($r^2$ = 0.98 and RMSE = 0.002431) in comparison to other existing predictors. [31-33], adopted an ANFIS-based approach for predicting the bed load for four moderately-sized rivers. While other equations failed to produce an accurate result, the ANFIS results showed an accurate prediction for measured bed-load data based on a regression method used for comparison.

This research is aimed at proposing an ANFIS model capable of utilising five input parameters in determining the volume of sediment deposited in Ikpoba dam and the amount not reaching the dam at the time when observations were conducted tagged "sediment-loss-in-transit" (SLIT). The model design links the input parameters to aggregate the devastating effect of sediment volume intake of the dam which contribute significantly to early loss of storage capacity. Sediment evaluation at the dam based on the quantity of soil loss from gully erosion transported through the river channel can serve as guide to the water resource managers, hydraulic engineers, and dam operators in taking appropriate decisions on dam water-sharing routine, dam useful life monitoring, dam rejuvenation efforts, cost-effective sediment remediation method, dam management planning, and so on.

## 2. Materials and Methods

### 2.1. Study area

The study area captured the upstream part of the Ikopba River dam where two prominent gullies, namely, (the University of Benin gully and the Iguosa-Oluku gully) are exiting their massive sediment into the Ikpoba river channel within the same catchment in Benin City, Edo State, Southern Nigeria. The geographical location of the study area falls within UTM Zone 31N, 789050.75 mE; 705200.22 mN, and 795500.96 mE; 715950.26 mN). By Koppen classification, Benin City has a tropical savanna climate with rainfall intensities reaching up to 2680mm annually in most cases. The rainfall lasts between eight to nine months, starting in March through October at varying degrees, resulting in a substantial amount of overland flow with impactful erosive energy. The average annual temperature at this location was 25.6 °C. The Benin City region is characterized by the sedimentary formation underlay of what is called the "South Sedimentary Basin," with the geology marked by the presence of reddish earth on top, composed of ferruginized or literalized clay sand [34]. The geologic formations in the region are classified into four basic categories: the Benin formation; alluvium; drift/topsoil and Azagba-Ogwashi. The type of soil in this region, which has low cohesive aggregate binding force, is highly susceptible to erosion influence, therefore gully formation is always prevalent. The study area including the immediate catchment is shown in Figure 1.

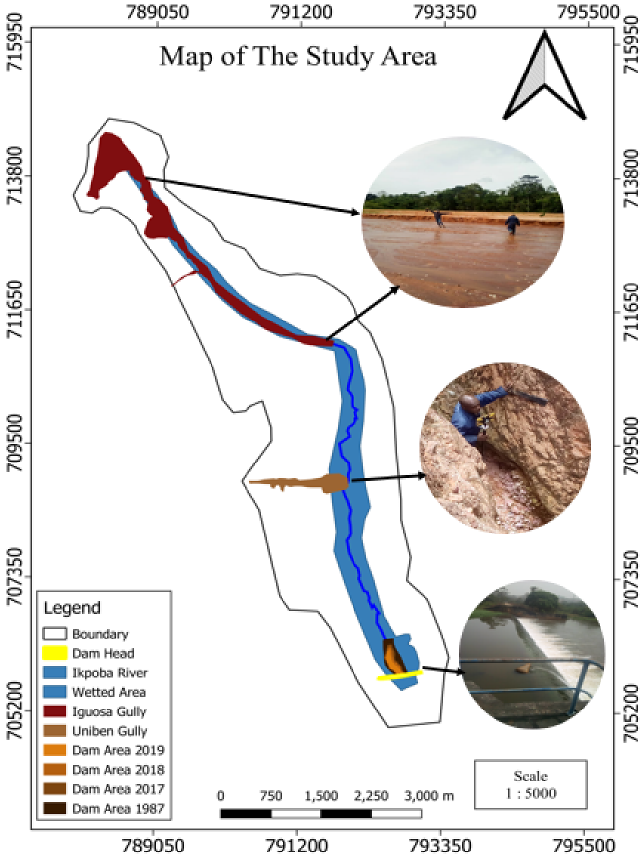


Figure 1. Map showing the study area

## 2.2. The Description of the Gullies

The University of Benin gully and the Iguosa-Oluku gully hereafter referred to as gully (A) and gully (B), respectively, are located in the upper part of the Ikpoba dam. Although there is no specific documentation on the exact date on which Gully (A) began, it started earlier than the year 2005 as captured by Google Earth historical images. Its development has caused some buildings to be completely or partly eroded at the senior staff quarters of the University due to the gradual landslide resulting in gully sidewall collapse. The guest house of the University is presently under threat. Figure 2 reveals the impacts of gully erosion on some properties and the immediate surroundings of the invested environment.

According to an anonymous resident, the rehabilitation of the Benin/Lagos expressway in 2014 caused the start of the gully (B). Its initiation and subsequent development are tied to the volume of run-off diverted to a drainage system not appropriately designed to convey such an amount. Hence, the water created an alternative path across the existing settlement, actively creating a bigger and deeper channel. Six years of no visible remedial intervention led to the destruction of more than fifty buildings, including a police station and other utilities. The Federal housing estate located close to where the gully extension has reached is now in grave danger of being eroded. Figure 3 shows the devastation caused by gully erosion (left) and the massive soil loss deposited along the Ikpoba river course (right).

Table 1. Construction information of Ikpoba dam

| S/No | Name of Dam: Ikpoba | Remark |
|---|---|---|
| 1 | Type of Dam | Earth fill |
| 2 | Water production per pump day | 34080 $m^3$ |
| 3 | Catchment area | 120 $km^2$ |
| 4 | Crest level height | 35 m (a.m.s.l) |
| 5 | Dam length | 610 m |
| 6 | Active storage capacity | $1.5 \times 10^6$ $m^3$ |
| 7 | Reservoir surface area | $1.07 \times 10^6 m^2$ |
| 8 | Service spillway length | 60 m |
| 9 | Emergency spillway length | 4 m |
| 10 | Water supply capacity | 90,000 $m^3$/day |
| 11 | Average monthly discharge | 31.9$m^3$/s |
| 12 | Average annual run-off | $0.9285 \times 10^9 m^3$ |
| 13 | Population at design | 1.0 million |
| 14 | First impoundment year | 1975 |
| 15 | Commission year | 1987 |

Source: [38]

## 2.3. Description of Ikpoba river and dam

The Ikpoba River originated from the Oluku settlement area in an extension of Benin City's western highland towards the northern and north-eastern parts [35]. From the identified source, the river flows from east to west; reverses its course and meanders through Utekon before changing direction to the southern and eastern banks through the following axes (Ekosodin, Ugbowo, Okhoro, and New Benin). The river has some level of interactions with the exited sediment from the gullies under consideration. The Ikpoba dam is an earth dam that is located along the river reach between Okhoro and Teboga. It is a small dam according to the classification of the International Commission on Large Dams [36]. The construction work of the dam began in 1977 and was commissioned in 1987. The Benin-Owena River Basin of Nigeria manages the dam in conjunction with the Edo State Urban Water Board. The geological terrain is tertiary and the foundation is pile-based. Four stations are present before reaching the dam's head [34-37]. These are (Okhoro, Midpoint, Low-lift pump, and Ekiuwa). According to [38], the dam has a length of 610 meters. Table 1 provides useful information on the physical characteristics and parameters of the dam.

## 2.4. Gully data acquisition and Preparation

A Trimble M3 DR 3" Total Station and a Trimble Juno 3B handheld GNSS receiver were used for data collection. Existing ground controls on sites were subjected to an integrity test and found to be stable before proceeding to observations. The cross-sectional design was done in AutoCAD civil 3D for 2017, 2018, and 2019, respectively. Samples are presented in Figure 4. The volume of each gully segment at chainage 20m apart was computed by the average area of the up and downstream cross sections multiplied by their respective segment lengths.

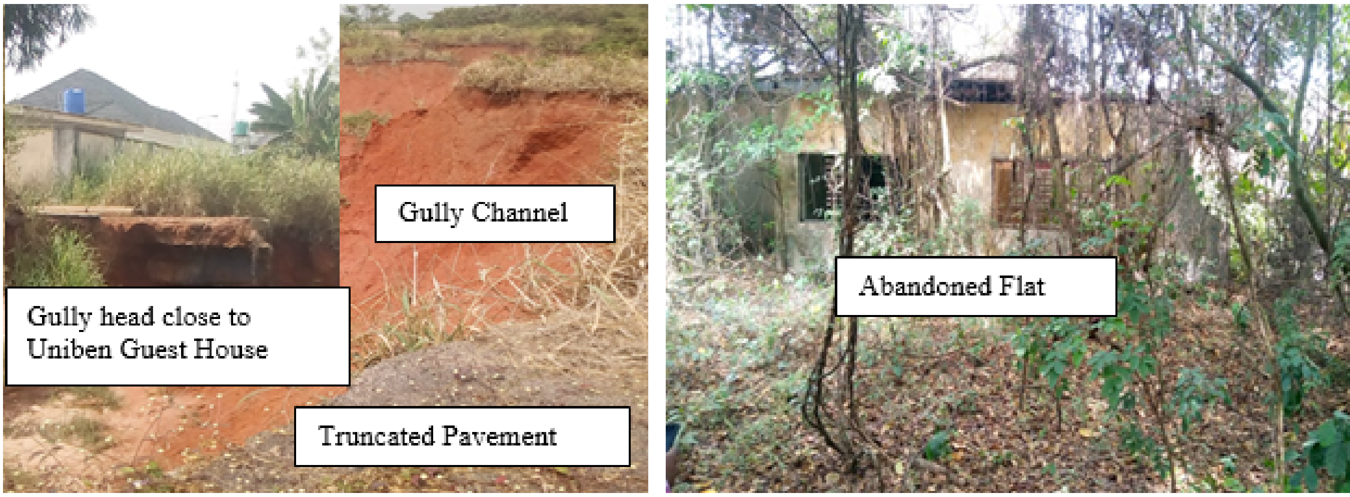


Figure 2. Gully (A) and its negative impacts on settlement

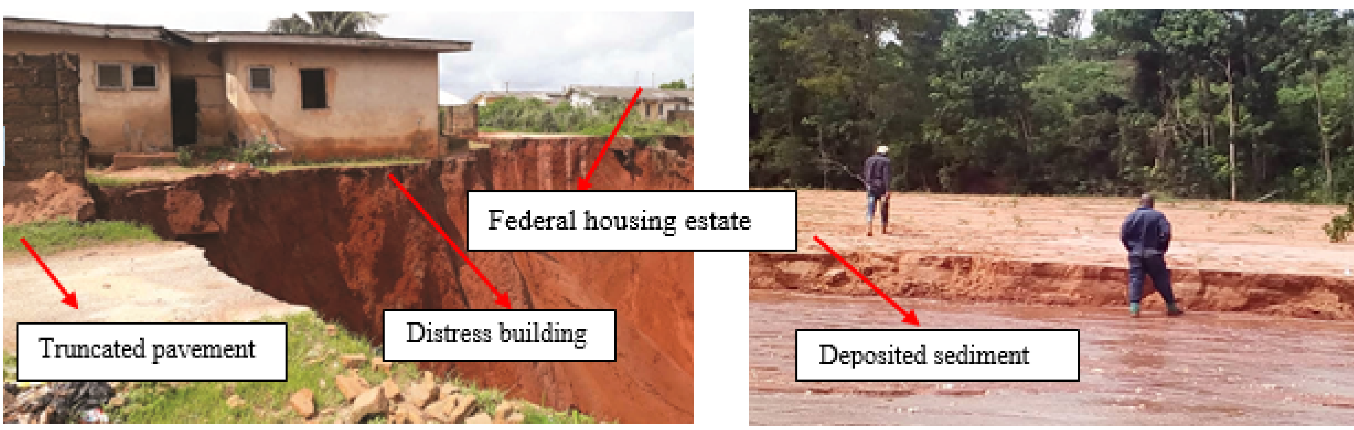


Figure 3. Devastating impact and soil loss from Gully B

The cumulative sum of all sectional volumes represents the total sediment volume contributed by gullies. See Table 2.

### 2.5. *Bathymetric data acquisition and preparation*

The bathymetric surveys of the reservoir were conducted in 2017, 2018, and 2019, respectively. The procedure involved the coupling of the 15-HP Yamaha engine to the fiber boat and pushing it away from the bank to gain enough depth to allow for the attachment of the transducer and the mounting of the GNSS receiver firmly to their respective positions. The position fixing was done in RTK mode using the Hi-Target GNSS receiver while depths were measured simultaneously with the aid of the Hi-Target Marine HD-Max Echo Sounder powered by a 12-volt battery. The appropriate bar checks were observed against the standard marks at 1 m, 2 m, and 3 m for consistency and the eradication of false depth records. This check was done before and after the bathymetric surveys. Twenty-five transect lines (25) and two longitudinal cross lines (2) were traversed. The output from the RTK-GNSS receiver are precise 3-D (X, Y, Z) coordinates with obtained accuracies in the order of 0.02m for horizontal and 0.05m for vertical, respectively. Corrections for pitch roll and heave were applied at the software interface on board to get the corrected depths. During the different campaigns, water level monitoring was performed by planting a levelling staff at the bank of the river, and readings were taken with the aid of Nikon Automatic AC-2s leveling instrument before and after the bathymetric surveys. For the three campaigns, the average water level recorded at the beginning of work was 3.360m and at the end of work, it was 3.361m. The difference gave 0.001m. This result showed that the water at the dam was non-tidal and relatively calm throughout the time of observations. Note, that water level measurement may not pose a problem with the RTK technique, but when it is taken, it can be used for verification or validation purposes. We computed the volume of sediment accumulated in the dam using equation 1 [39]. Table 2, contains the technical parameters of the Hi-Target Marine HD-Max Echo Sounder, while Table 3 provides the summary of the total volume of sediment accumulated in the dam for the three years investigated. Figure 5 shows

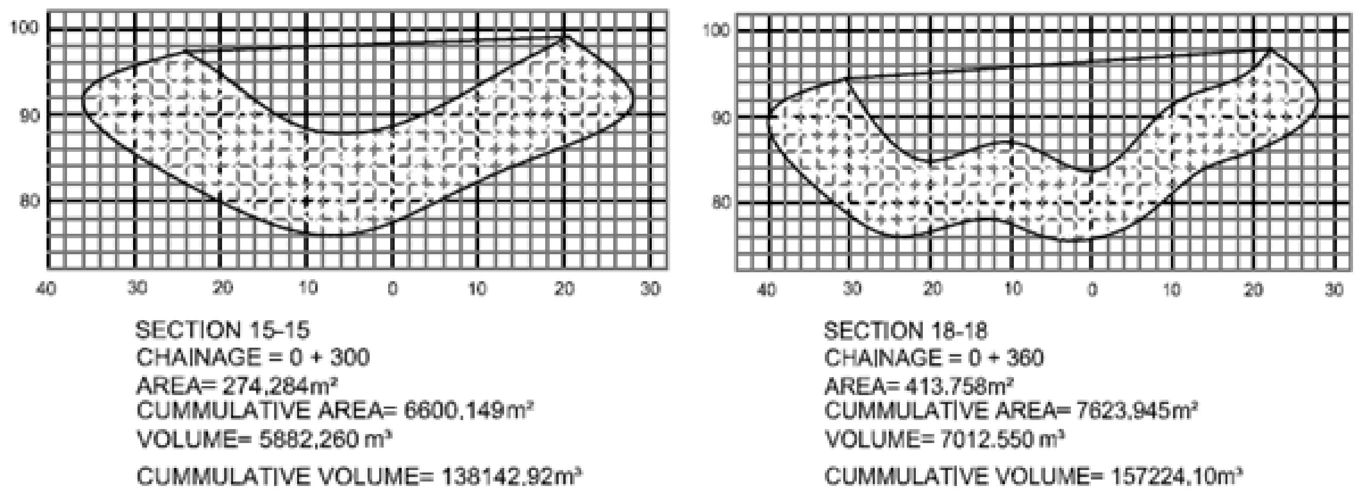


Figure 4. Sample of cross-sectional design for gullies

Table 2. Summary of calculated volume of sediment from Gullies

| Year | Gully_ID | Vol. loss ($m^3$) | Cumulative Vol. loss ($m^3$) | Total Vol. ($m^3$) |
|---|---|---|---|---|
| 2017 | | 256791.548 | 000000.000 | |
| 2018 | A | 268363.430 | 525154.978 | |
| 2019 | | 277543.350 | 802698.328* | 802698.328 |
| 2017 | | 375478.830 | 000000.000 | |
| 2018 | B | 414810.690 | 790289.520 | |
| 2019 | | 475275.954 | 1265565.474* | 1265565.474 |
| **Grand Total** | | 2068263.802 | 2068263.802 | 2068263.802 |

**Note:** **are the **o**nly final yearly volumes considered in column 4 for to get the grand total

the water level monitoring effort at the dam's location.

$$R_{annua} = \frac{V_1 - V_f}{T} \tag{1}$$

Where $R_{annual}$, represents the annual mean reservoir sedimentation volume in (Mm$^3$/year); $V_i$, refers to the initial reservoir volume in (Mm$^3$); $V_f$, signifies the final reservoir volume in (Mm$^3$); $T$, is the number of years since dam had been operated.

$$TVU = \pm\sqrt{a^2 + (b \times d)^2} \tag{2}$$

### 2.6. The ANFIS architecture

The input data, the hidden layers, and the output layer are the three fundamental components of the ANFIS architecture. The ANFIS model type used in this study is the Sugeno, with five layers. What necessitate its use was because of its compactness and efficient computational capability [42]. Instead of working with linguistic variables on the consequent part as in the Mamdani model, the TSK model [41-45] uses rules as a function of input variables to represent the consequent parts. Its success is due mainly to the ease of generating a set of system equations for the consequent parts, the parameters of which are simple to estimate using traditional optimization methods. However, the interpretation of the obtained rules is somewhat difficult, which shows their principal shortcoming. The TSK learning algorithm consists of two processes, the forward and the backward stage. The forward phase goes through the five layers to be discussed after in text while the backward stage fine tune the weights of a neural network by using the error rate previous epoch [24]. In a first-order Sugeno fuzzy model, a typical fuzzy rule statement takes the form of say Where: A and B are fuzzy sets in the antecedent, is a crisp function in the consequent. The five layers are simplified further to briefly explain what takes place at each layers of the ANFIS model.

**(i) Layer-1**

This layer is the first, and is very critical to the overall process. Equations 3 or 4 represent what takes place at this phase [42].

$$O_{1,}i = \mu A_i(x) \quad \text{for} \quad i = 1, 2 \tag{3}$$

or

$$O_{1,}i = \mu(B_{i-2})(y) \quad \text{for} \quad i = 3, 4 \tag{4}$$

Where: $x$ or $y$ -represents the input taken by node $i$, $A_i$ or $B_{i-2}$ -signifies a form of linguistic descriptions (e.g. high, low

Figure 5. Bathymetric survey and water level monitoring exercise at Ikpoba dam

Table 3. Technical parameters of HD-MAX Echo Sounder

| **S/No** | **(a) Technical parameters** |
|---|---|
| 1 | CPU speed: 1.6G*2 |
| 2 | RAM: 2GB |
| 3 | Memory space: 16GB SSD |
| 4 | Display screen size: 17” |
| 5 | Display resolution: 1280*1024 |
| 6 | Starting time: < 40s |
| 7 | High frequency emitted from the probe: 200KHZ |
| 8 | Point-positioning precision: <2.5M (built-in GPS function) |
| 9 | Input voltage: 10 30V |
| 10 | Average power consumption: <40W |
| 11 | Operating temperature: 0 50°C |
| | **(b) Bathymetric Accuracy** |
| 12 | Horizontal = 0.506m, at 95% confidence level. |
| 13 | Vertical = 5m + (-0.30m) at 95% confidence level. |

Note: We applied the formula provided by the International Hydrographic Organisation, [40] for the determination of horizontal and vertical uncertainties in depth measurement. The maximum depth obtained during sounding was 6.0m, while *a* and *b* are constants provided for in the formula. To compute total horizontal uncertainty, we used, THU = 5m + 5/100 of depth. Equation 2 was used to compute the total vertical uncertainty, TVU. The results are contained in the last two rows of Table 3.

and so on) assigned to node $i$, $O_1,i$ -represents the membership function of fuzzy set $A_i$ which signifies the extent to which the input $x$ or $y$ under consideration satisfies the quantifier $A_i$. $\mu A_i(x)$ and $\mu B_{i-2}(y)$ can accommodate any fuzzy membership function assumed to spread between 0 and 1.

For example, if the bell-shaped membership function is adopted, $\mu A_i(x)$ follows the equation 5

$$\mu A_i\,(x) = \frac{1}{1 + \left[\left(\frac{x-c_i}{a_i}\right)^2\right] b_i},\ i = 1, 2 \tag{5}$$

Table 4. Summary of calculated volume of sediment in Dam

| Year | Ikpoba Dam | Annual Sed. Vol. ($m^3$) | Cumul. Sed. Vol. ($m^3$) | Comp. Bed-load Sed. Vol. ($m^3$) |
|---|---|---|---|---|
| 1987 | Base year | N/A | 000000.000 | |
| 2017 | $1^{st}$ Observation | 217336.704 | 217336.704 | |
| 2018 | $2^{nd}$ Observation | 222790.642 | 440127.346 | |
| 2019 | $3^{rd}$ Observation | 400000.000 | 840127.346* | |
| **Grand Total** | | **840127.346** | **840127.346** | **840127.346** |

Note:*is the only one considered under column 4 for the ground total

Where: $a_i$, $b_i$, and $c_i$ in equation 5 are the premise parameters set of the generalized bell shape membership function (MF).

The current study adopted the Gaussian membership function (MF) defined by equation 6.

$$\mu A_i(x) = exp\left[-\left(\frac{x-c_i}{a_i}\right)^2\right] \quad (6)$$

Where: $a_i$ and $c_i$ in equations 6 are the premise parameters set of the Gaussian MF.

Changing the values of these parameters would cause a corresponding change in the generalize bell-shape behaviour and the Gaussian shape that will make the fuzzy set "$A_i$" to exhibit various forms of membership functions. In this layer, parameters are commonly called premise parameters [42- 45].

**(ii) Layer-2**

At this layer, each ANFIS node represents a fixed node with an output signal as the product of the contributions of the incoming signals.

$$O_{1,}i = w_i = \mu A_i(x) * \mu(B_{i-2})(y), \quad for \quad i = 1, 2 \quad (7)$$

Each node output in this context is a representation of a rule's firing strength capacity. The node function in this layer will typically be any other T-norm operator that can execute fuzzy (AND). **(iii) Layer-3**

This layer has a fixed node labeled *N*. Here, the $i^{th}$ node computes the ratio of the $i^{th}$ rule's firing strength to the sum of all rules' firing strengths. The outputs of this layer are the normalized firing strengths, represented as follows:

$$O_3, i = \overline{w}_i = \frac{w_i}{w_1 + w_2} \; : for \; i = 1, 2. \quad (8)$$

**(iv) Layer-4**

Every node *i* contained in this layer represents an adaptive node with a node function:

$$O_4, i = \overline{w}_i f_i = \overline{w}_i(p_i x + q_i y + r_i), \quad (9)$$

Where: The ANFIS in this layer represents a normalized firing strength inherited from layer-3, and the quantities represented as: ($p_i$, $q_i$ and $r_i$) are the parameters set of this node. Parameters here are termed consequent [41- 45].

**(v) Layer-5**

This layer is an ANFIS with a fixed node label and a single node that sums all incoming signals to produce the overall output:

$$O_5, i = \sum_i \overline{w}_i f_i = \frac{\sum_i w_i f_i}{\sum_i w_i} = the\ overall\ output \quad (10)$$

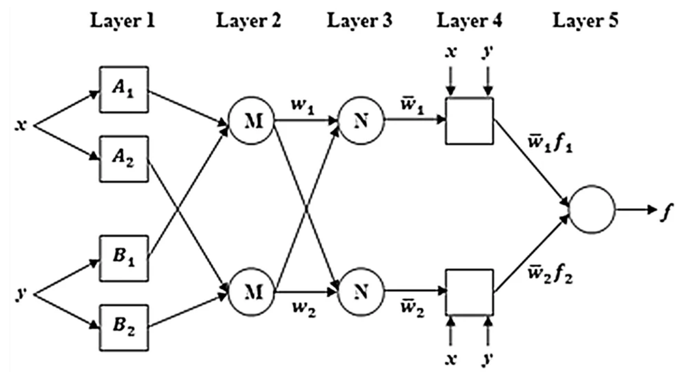


Figure 6. ANFIS architecture. Source: [41]

These five steps simplify a functional Takagi-Sugeno fuzzy model for an adaptive network design.

The backward stage is a useful process in estimating the database; this consists of the parameters of the membership functions in the antecedent part and the coefficients of linear equations in the consequent part. The least-squares method assists greatly in parameter learning by utilizing standard fuzzy reasoning to anticipate the outcome of the TSK model in the prediction phase [41- 45]. Figure 6 shows the ANFIS architecture.

### 2.7. Description of ANFIS input parameters

The parameters used for the ANFIS model contain the five most important site-specific variables that are either observed, measured, or determined through laboratory analysis for the study area. ***Rainfall:*** Rainfall data were collected using two tipping bucket rain gauges located within the catchment of the Ikpoba river close to where gully A and gully B exit their sediment into the river channel in conjunction with rainfall data obtained from the Nigerian Meteorological Agency (NiMet). The collected rainfall data was used for validation. The data was resampled and gridded to 220 to comply with the gully cross-section.

***Volume:*** For the three years specified earlier, gully A and gully B had 109 and 111 cross-sectional segments, adding up to 220 for which volumes of sediment were calculated and cumulated to derive the cumulative volume of sediment deposited.

***Slope:*** The slope length was determined as run over the rise at each gully cross-section. The depth of gullies taken at each cross-sections varied from 6.0 m to 11.23 m.

***Particle size:*** Particle size was obtained from soil samples taken at 1m to 3m from 20 borehole points dug with a hand huger at the two gully sites. Sieve analysis was carried out at the University of Benin Civil Engineering Laboratory.

***Velocity:*** The velocity was measured manually at pre-defined sections along the gullies on rainy days. The widths were measured with 100 m graduated steel tape, and the upper and lower boundaries of each section were defined with wooden pegs wrapped with caution tape. This information was recorded and kept for further use. On two different rainy days, a floating material (cork) was released from the gully's head and the time taken for it to travel between the flags was recorded with a stopwatch. Five observers were stationed in succession to record time with a stopwatch until the process was completed. To find the velocity in (m/s$^2$), we divided the distance traveled by the average travel time and multiplied the result by a chosen correction factor of 0.9 which is mostly adopted for rivers or flowing water whose bottom consists of smooth mud, and sand, or bedrock.

The summary of the description of the ANFIS input parameters in terms of their minimum and maximum limits and their respective membership functions is presented in Table 5. Each parameter has three (3) membership functions.

### *2.8. Preliminary investigation on input parameters*

Ordinary least squares (OLS) regression models on sediment volume retained all covariates with $p<0.05$, explaining 93.8% variability in the dataset. Assessment of the multicollinearity related to the dataset using the variance inflation factor was found not to pose a problem (VIF<5) obtained throughout for covariates is sufficient [46-49].

### *2.9. Data normalisation*

Avoiding data normalisation may lead to a complex situation in the training process and non-convergence of the algorithm. The min-max normalisation technique that scales the variables in the interval between (0, 1). The data was randomised (the purpose is to reduced bias and make the output more reliable). The data was further divided into training and testing datasets after normalisation. After making a good number of data sharing attempts by trial and error, the choice of 75% was made and used for training, while the remaining 25% was used for testing. This sharing ratio gave the optimal result and accuracy compared to others where less or greater value of sharing resulted in large error. The training data performed the role of the ANFIS training process and the generation of the fuzzy rule-based systems (FRBS), whereas, the testing data served the purpose of verifying the accuracy and effectiveness of the trained ANFIS model. For efficient ANFIS processing, the input dataset used was processed in a data frame in form of a matrix ($m \times n$), where **m** is the number of instances, **n** is the number of variables, while the last column in the matrix represents the output. Tables 6 and 7 are excerpts from the normalized training and testing data respectively.

### *2.10. Training process*

The process began by obtaining a training data set (input/output data pairs) and checking of the data sets. Two vectors are used to train the ANFIS system: the input vector and the output vector. ANFIS training rules used was a hybrid learning, which combines the gradient descent and the least-squares method. The training proceeds by determining the fuzzy sets and the number of sets for each input variable and the shape of their membership function. All the training data passes through the neural network, to adjust the input parameters so as to find the relationships between input/output, and to minimize errors propagation. The parameters associated with each membership function kept changing throughout the learning process and a threshold value for the error between the actual and the desired output was determined. If the error is larger than the set threshold value, then the premise parameters are updated using the gradient descent method. The consequent parameters are found using the least-squares method. The process is terminated when the error becomes less than the threshold value. We used the checking data set to compare the model with the actual system.

The input node received signals from each of the five predictor nodes, connected through intervening hidden nodes. Above each line is the displayed of the respective synoptic weights. The blue circles indicate bias, corresponding to the intercept in the conventional regression model. The variable "*sediment volume"* represents the output neuron. The network converged when the error reached 0.190791, after 417 steps. The mathematics involved in this process is shown in equations 11 and 12. Figures 7 and 8 show the ANN network topology and the flow diagram of the ANN training process, respectively.

$$w_{ij}(t+1) = w_{ij}(t) + \eta\delta_{pi}O_{pj} \tag{11}$$

$$\delta_{pi}w_{ij}(t+1) = w_{ij}(t)+\eta\delta_{pi}O_{pj}+\alpha\left[w_{ij}(t) - w_{ij}(t-1)\right] \tag{12}$$

Where:

Weight coefficient in step *t+1*, from neuron *i* to neuron *j*

Weight coefficient in step *t*, from neuron *i* to neuron *j*

: learning Coefficient

: Difference between desired output and network output in neuron *p* of layer *j*

: Output of neuron *p* of layer *j*

: Momentum coefficient

: Weight coefficient in step *t-1*, from neuron *i* to neuron *j*.

### *2.11. Model validation metrics*

In this work, model validation was carried out using the Mean Squared Error (MSE), the Mean Absolute Error (MAE), and the correlation coefficient (r). For simplicity of use, ease of training, and better performance, the rectified linear unit (ReLU) activation function was used. It is a piecewise linear function that will output the input directly if it is positive, otherwise, it will output zero. Equations 13 - 15 are the statistical models adopted in model validation.

$$RMSE = \sqrt{\frac{\sum_{i=0}^{N}(d_i - y_i)^2}{N}} \tag{13}$$

$$r = \frac{\frac{\sum(y_i-\bar{y})(d_i-\bar{d})}{N}}{\frac{\sqrt{\sum_i(d_i-\bar{d})^2}}{N}\frac{\sqrt{\sum_i(y_i-\bar{y})^2}}{N}} \tag{14}$$

Table 5. Brief description of input parameters

| | Gully A (109 C.S) | | Gully B (111 C.S) | | = 220 |
|---|---|---|---|---|---|
| Parameters | Min. | Max. | Min. | Max. | MF |
| Rainfall (mm) | 55.85 | 104.49 | 167.80 | 215.70 | 3 |
| Slope-length (m) | 29.89 | 71.99 | 30.85 | 63.27 | 3 |
| Depth (m) | 6.45 | 11.23 | 4.70 | 9.61 | 3 |
| Velocity (m/s) | 0.51 | 1.84 | 0.44 | 1.86 | 3 |
| Particle Size (µm) | 28.77 | 41.69 | 34.85 | 47.90 | 3 |
| Gullies Sed.Vol. x $10^4$ ($m^3$) | 5651 | 8473 | 8652 | 13370 | 3 |

**Note:** C.S = Cross-section, MF = Membership Function

Table 6. Excerpt from normalised training data

| index | Rainfall(mm) | Slope(mm) | Depth(mm) | Velocity(m/s) | P.size(µm) | Volume($m^3$) |
|---|---|---|---|---|---|---|
| 139 | 0.952312 | 0.325011 | 0.398463 | 0.514887 | 0.60261 | 0.673596 |
| 98 | 0.003783 | 0.286023 | 0.533673 | 0.78711 | 0.373132 | 0.220773 |
| 112 | 0.785692 | 0.205318 | 0.206067 | 0.396444 | 0.645918 | 0.756984 |
| 144 | 0.979885 | 0.646603 | 0.443222 | 0.099204 | 0.763262 | 0.900655 |
| 126 | 0.864056 | 0.298648 | 0.32029 | 0.365815 | 0.673003 | 0.817199 |
| 209 | 0.869185 | 0.089084 | 0.251222 | 0.281811 | 0.753548 | 0.860469 |
| 35 | 0.269768 | 0.842347 | 0.693181 | 0.1207 | 0.446288 | 0.236462 |
| 123 | 0.818387 | 0.622698 | 0.445846 | 0.925704 | 0.610277 | 0.618824 |
| 177 | 0.819464 | 0.238152 | 0.499117 | 0.182115 | 0.509774 | 0.612393 |
| 212 | 0.840235 | 0.554263 | 0.499378 | 0.074061 | 1 | 1 |

Table 7. Excerpt from normalised test data

| index | Rainfall(mm) | Slope(mm) | Depth(mm) | Velocity(m/s) | P.size(µm) | Volume($m^3$) |
|---|---|---|---|---|---|---|
| 7 | 0.214163 | 0.958774 | 0.722309 | 0.520943 | 0.491623 | 0.271775 |
| 109 | 0.074786 | 0.497832 | 0.675136 | 0.925770 | 0.395535 | 0.190251 |
| 140 | 0.883963 | 0.322317 | 0.279409 | 0.314403 | 0.804152 | 0.706681 |
| 74 | 0.136978 | 0.710343 | 0.793520 | 0.452986 | 0.266164 | 0.117517 |
| 205 | 0.725127 | 0.308324 | 0.531787 | 0.103523 | 0.842459 | 0.869096 |
| 111 | 0.753561 | 0.242328 | 0.000000 | 0.000000 | 0.548667 | 0.693910 |
| 187 | 0.812660 | 0.211266 | 0.441200 | 0.466538 | 0.485644 | 0.623276 |
| 100 | 0.152822 | 0.205663 | 0.491521 | 0.274293 | 0.426886 | 0.261896 |
| 189 | 0.892676 | 0.359164 | 0.323424 | 0.951899 | 0.597544 | 0.580190 |
| 88 | 0.237729 | 0.535238 | 0.651543 | 0.947341 | 0.349382 | 0.198406 |

$$MAE = \frac{1}{N}\sum_{N}^{j=1}|y_i - \hat{y}_i| \qquad (15)$$

Where:
$d_i$ : Desired output of *i-th* data
$y_i$ : Network output of *i-th* data
N: Number of dataset
$\bar{d}$ : Mean of desired output
$\bar{y}$ : Mean of network outputs
RMSE: Root Mean Square Error
MAE: Mean Absolute Error
$r$: Correlation coefficient

The summary of the investigated neural network algorithms presented in Table 5 shows that:

i.) All models have two hidden layer-nodes (5, 3) with ReLU activation function

ii.) The learning rule used for model 1 (NN-1) is resilient backward propagation.

iii) Levenberg algorithm was adopted for model 2 (NN-2), while

iv) Backward propagation algorithm was adopted for model 3 (NN-3).

A model that meets all the required evaluation criteria would be the desired model. Therefore, the model with the least RMSE and MAE errors (approaching 0) and the coefficient of determination "r" (tending to 1) obtained from NN-3 as highlighted in Table 8 is the most acceptable network result chosen. The predictive capability of the best model has an RMSE of **0.0423** with an $R^2$ of **0.947.** Table 9 shows the random points to demonstrate normalised and de-normalised for the training and testing datasets.

Table 9 presents the comparison of the actual test data and their predicted values based on the fitted training model. The

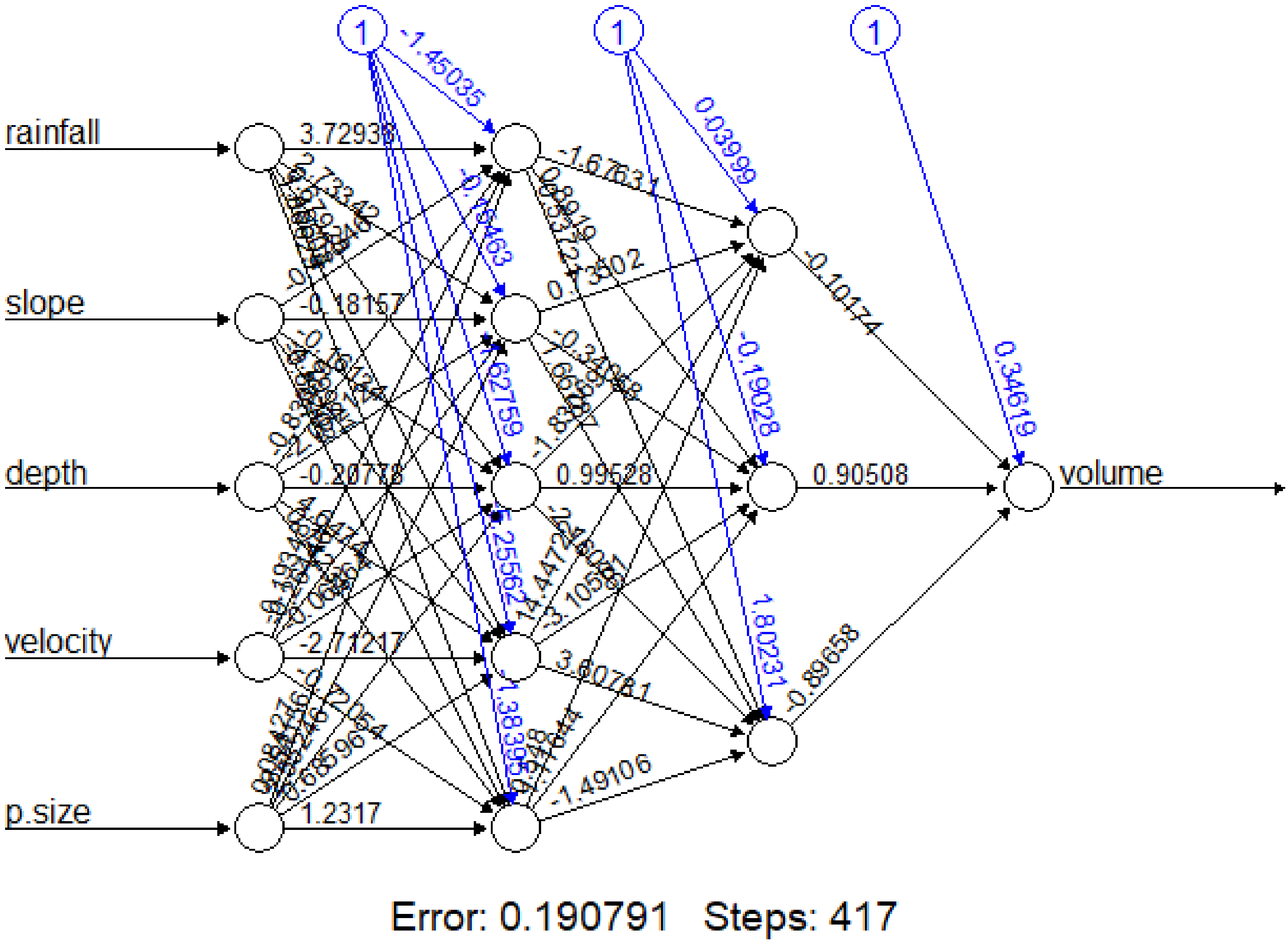


Figure 7. ANN training network topology

Table 8. Summary of Network Algorithms

| | | | | | Training | | | Test | | |
|---|---|---|---|---|---|---|---|---|---|---|
| **Model** | Hidden Layer | Nodes | Activation Function (F) | Learning Rule | MAE | RMSE | r | MAE | RMSE | r |
| **NN-1** | 2 | 8 | ReLU | Resilient back-propagation (rprop+) | 0.755 | 0.578 | 0.903 | 0.785 | 0.594 | 0.916 |
| **NN-2** | 2 | 8 | ReLU | Leverberg Algorithm | 0.644 | 0.546 | 0.924 | 0.687 | 0.548 | 0.919 |
| **NN-3** | **2** | **8** | **ReLU** | **Backpropagation (backprop)** | **0.0456** | **0.059** | **0.944** | **0.048** | **0.0423** | **0.947** |

remaining 25% of input parameters from the test data were fed into the trained ANFIS model to predict the output. It can be observed from the table that the predicted values were close to the original test data. The error rarely exceeds 10%, so the model was able to predict with an acceptable accuracy.

The regression plot in Figure 9 (left) displays the network outputs concerning the training and test data. For a perfect fit, the data should fall along a 45-degree line, where the network outputs are equal to the targets. For this particular problem, the fit is reasonably good for all data sets, with a trained coefficient of determination ($R^2$) value in each case of 0.947. Figure 9 (right) depicts the ANFIS training versus validation plot for the test dataset. A close overlap implies a high predictive power of the trained model on the new dataset. i.e., the predicted (purple

Table 9. The predictive power of the model on test data

| | **Normalised** | | **De-normalised** | | |
|---|---|---|---|---|---|
| Randomized Index | Actual | Predicted | Actual | Predicted | %error |
| 7 | 0.2718 | 0.2676 | 7748.541 | 7716.455 | 0.414 |
| 109 | 0.1903 | 0.1923 | 7119.224 | 7135.055 | -0.222 |
| 140 | 0.7067 | 0.8422 | 11105.789 | 12152.114 | -9.421 |
| 74 | 0.1175 | 0.1527 | 6557.752 | 6829.093 | -4.138 |
| 205 | 0.8691 | 0.7942 | 12359.551 | 11781.385 | 4.678 |
| 111 | 0.6939 | 0.6133 | 11007.203 | 10385.319 | 5.650 |
| 187 | 0.6233 | 0.5879 | 10461.952 | 10189.188 | 2.607 |
| 100 | 0.2619 | 0.2948 | 7672.287 | 7926.644 | -3.315 |
| 189 | 0.5802 | 0.6580 | 10129.345 | 10729.688 | -5.927 |
| 88 | 0.1984 | 0.2140 | 7182.175 | 7302.460 | -1.675 |
| 186 | 0.6273 | 0.7331 | 10492.945 | 11310.069 | -7.787 |
| 137 | 0.7870 | 0.8188 | 11725.892 | 11971.350 | -2.093 |
| 32 | 0.1499 | 0.2065 | 6807.912 | 7244.302 | -6.410 |
| 71 | 0.2234 | 0.2255 | 7375.058 | 7391.463 | -0.222 |
| 210 | 0.7040 | 0.6087 | 11084.715 | 10349.643 | 6.631 |

line) has 94.7% predictive accuracy as reported from the value of $R^2$. The attained training error for the test model is obtained as 0.0423.

## 3. Results and Discussions

### *3.1. Sediment deposit in dam*

The total volume of sediment contributed for three years by gullies was 2068263.802 $m^3$. Similarly, the calculated volume of bed-load sediment gained by the dam was 840127.346 $m^3$ (refer to Tables 2 and 4). Here, we are faced with using the model to reproduce the amount of sediment deposited in the dam.

$$\text{Mathematical relationship: } V_{Gully} - V_{Transit} = V_{Dam} \quad (16)$$

Based on the preamble at the start of this sub-section.
Let,

$$2068263.802 V_{Gully} = 840127.346 V_{Dam}$$

Therefore,

$$V_{Dam} = \left(\frac{2068263.802}{840127.346}\right) \times \gamma$$

$$\Rightarrow V_{Dam} = 2.4618 V_{Gully}\gamma \quad (17)$$

Where: $\gamma$ is the smoothing parameter or correction factor with value ranging as $(0 < \gamma < 1)$.

$$\%Error = \frac{V_{DamPredicted}}{V_{Dam}} \times 100\% \quad (18)$$

Where: $V_{DamPredicted}$ refers to the expected volume of sediment obtainable at the dam that would correspond to the volume computed and $V_{Dam}$ is the final volume calculated at the dam's end.

The smoothing parameter is the correction term applied to correct unmeasured external factors such as channel gradient, channel roughness, or corrosion. It helps in computing the volume of sediment in the dam for every combination of hyperparameters specified by evaluating against a specified (Dam volume constant of 840127.346 $m^3$). The appropriate value of the correction factor can either be learned by trials and error or through cross-validation. This study adopted a cross-validation sequence combining (0.1 and 0.2 step size of 0.005) for hyperparameters. Table 10 showed the percentage error and the predicted volume of the dam at each iteration of

Table 10, reveals the predicted volume of sediment by the ANFIS model. A grid search predicted value of 842895.8547 $m^3$ obtained at 0.165 yielded the best smoothing value for predicting volume of sediment present in the dam with a percentage error of -0.3295344%. The original volume of sediment computed at the dam was 840127.346 $m^3$ being used as constant all through. Initially, the error rate decreases as increases until it attains an optimal value of 0.165. By iterating beyond this value, the error rate starts increasing in the opposite direction.

### *3.2. Sediment Loss-in-Transit*

Sediment loss-in-transit per-unit volume is the difference between the calculated amount of sediment exited (deposited) from the gullies and the amount of sediment gained by the dam. This concept forms the basis of the proposed model. Equation 18 expresses another form of equation 15, obtained by making the volume of sediment loss-in-transit the subject of the formula of the relation. The deduction from the model shows that it is capable of estimating the computed volume of sediment loss-in-transit by using Equation 19.

$$V_{Transit} = V_{Gully} - V_{Dam} \quad (19)$$

Total volume of soil loss (sediment) from gully = 2068263.802 $m^3 = V_{Gully}$

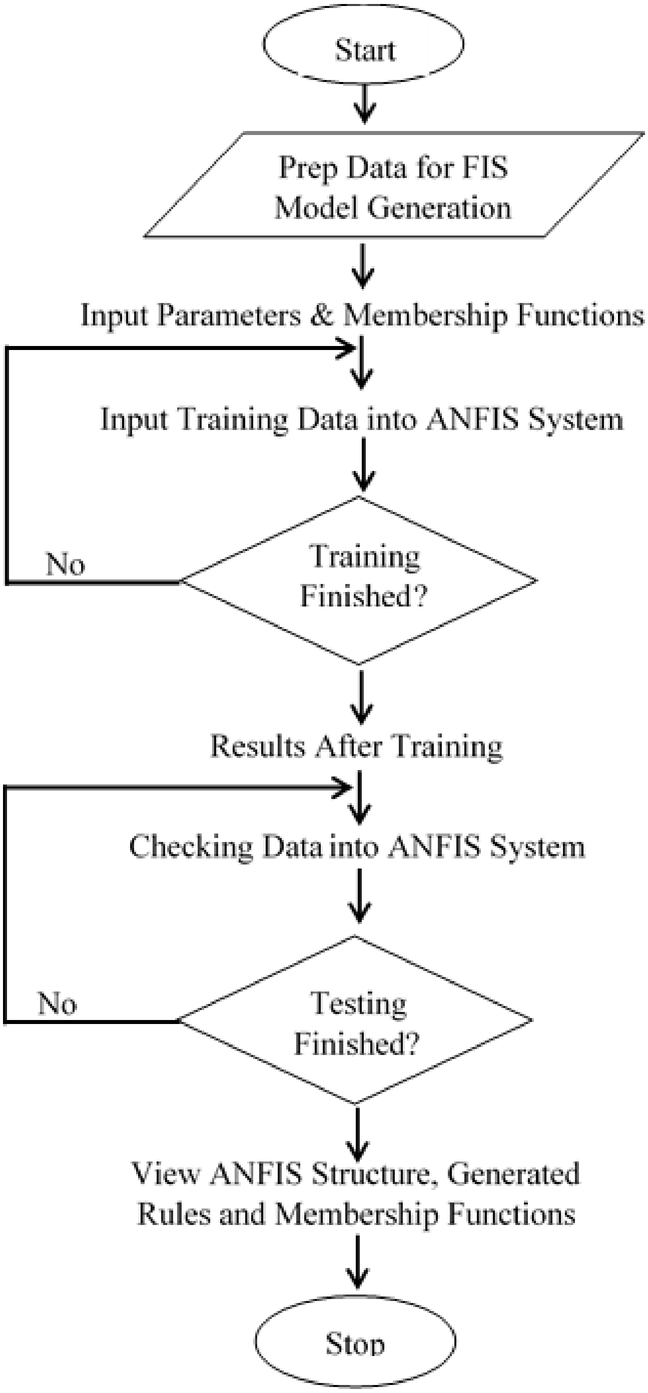


Figure 8. Flow diagram of ANFIS training process

Total volume of bed-load sediment gained by dam = 840127.346 $m^3 = V_{Dam}$
Total volume of soil loss-in-transit (difference) = 1228136.456 $m^3 = V_{Transit}$

Note: the difference is the volume of sediment regarded as "loss-in-transit," which could not be accounted for at the dam's end during field campaigns. Therefore, we are faced with the task of using the model to predict the volume of (sediment) loss-in-transit given an array or matrix of input parameters.

The proposed ANFIS model was trained to reproduce the volume of sediment loss-in-transit at 10 randomly selected data points from the test data for (predicted gully volume and predicted dam volume) each, respectively. The results generated by the model for the predicted gully volume, the predicted dam volume, and the volume of sediment loss-in-transit including the final summation for each of the last three column variables are presented in Table 11.

Table 10. Percentage error and predicted volume of dam at each iteration of $\gamma$

| $\gamma$ | $V_{Dam}$ ($m^3$) | $V_{DamPredicted}$ ($m^3$) | %Error |
|---|---|---|---|
| 0.100 | 840127.346 | 510845.9726 | 39.19422157 |
| 0.105 | 840127.346 | 536388.2712 | 36.15393265 |
| 0.110 | 840127.346 | 561930.5698 | 33.11364373 |
| 0.115 | 840127.346 | 587472.8684 | 30.0733548 |
| 0.120 | 840127.346 | 613015.1671 | 27.03306588 |
| 0.125 | 840127.346 | 638557.4657 | 23.99277696 |
| 0.130 | 840127.346 | 664099.7643 | 20.95248804 |
| 0.135 | 840127.346 | 689642.0629 | 17.91219912 |
| 0.140 | 840127.346 | 715184.3616 | 14.8719102 |
| 0.145 | 840127.346 | 740726.6602 | 11.83162127 |
| 0.150 | 840127.346 | 766268.9588 | 8.791332352 |
| 0.155 | 840127.346 | 791811.2575 | 5.751043431 |
| 0.160 | 840127.346 | 817353.5561 | 2.710754509 |
| 0.165 | **840127.346** | **842895.8547** | **-0.3295344**** |
| 0.170 | 840127.346 | 868438.1533 | -3.369823334 |
| 0.175 | 840127.346 | 893980.452 | -6.410112256 |
| 0.180 | 840127.346 | 919522.7506 | -9.450401177 |
| 0.185 | 840127.346 | 945065.0492 | -12.4906901 |
| 0.190 | 840127.346 | 970607.3479 | -15.53097902 |
| 0.195 | 840127.346 | 996149.6465 | -18.57126794 |
| 0.200 | 840127.346 | 1021691.945 | -21.61155686 |

** - Optimum smoothing parameter

From the 11 randomly selected points tested, the was calculated using the mathematical relationship of equation 15. Hence, for a predicted gully volume of 97318.44 $m^3$, a calculated (predicted) volume of 39530.46 $m^3$ would be deposited in the dam. Then, predicted volume loss-in-transit is therefore given as (97318.44 - 39530.46) $m^3$ = 57787.98 $m^3$. This shows that the proposed model is capable of generation output for every instance where predicted gully sediment volume and dam's sediment volume exist.

## 4. Conclusion

This work was carried out to examine the capability of the ANFIS hybrid model to predict sediment volume supplied from upstream by two prominent gullies through the Ikpoba river channel and the amount of sediment accumulated (gained), as much as can be accounted for at the Ikpoba dam's end. Three-year consecutive field campaigns at the gullies' location and dam's end enabled us to prepare, refine, normalise, and modify the input parameters for optimum model performance.

We first applied the ANFIS model to reproduce the volume of sediment deposited in the dam as calculated and proposed a mathematical relationship that incorporated the ANFIS model

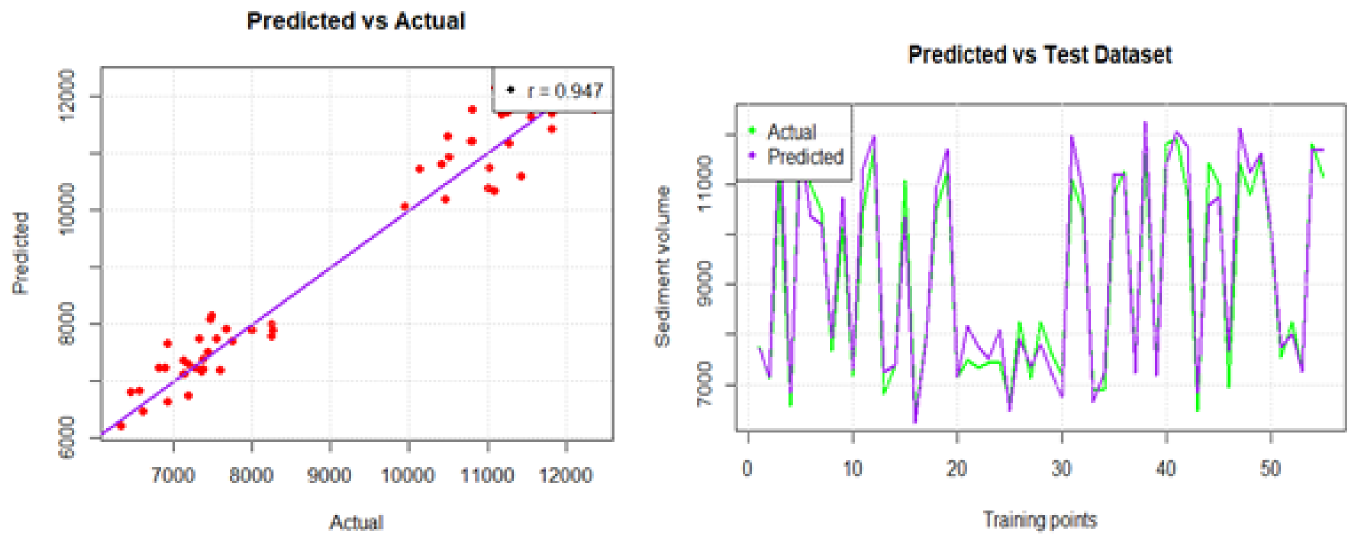


Figure 9. Regression (left) and Validation (right) plots

Table 11. Predicted volume loss-in-transit from a random selection of 10 data points

| index | Rainfall (mm) | Slope (mm) | Depth (m) | Velocity (m/s) | P. size (µm) | Volume ($m^3$) | Predicted Gully Volume ($m^3$) | Predicted Dam Volume ($m^3$) | Volume Loss-in-Transit ($m^3$) |
|---|---|---|---|---|---|---|---|---|---|
| 100 | 80.280 | 38.545 | 7.908 | 0.827 | 36.934 | 7672.287 | 7926.644 | 3219.779 | 4706.865 |
| 186 | 202.963 | 38.118 | 6.522 | 1.412 | 41.182 | 10492.945 | 11310.07 | 4594.116 | 6715.953 |
| 189 | 198.573 | 45.008 | 6.811 | 1.791 | 40.199 | 10129.345 | 10729.69 | 4358.367 | 6371.321 |
| 210 | 176.937 | 37.126 | 5.928 | 1.210 | 39.141 | 11084.715 | 10349.64 | 4203.994 | 6145.649 |
| 159 | 193.554 | 39.714 | 6.411 | 1.463 | 38.102 | 9951.850 | 10079.82 | 4094.394 | 5985.429 |
| 13 | 84.328 | 53.774 | 8.771 | 1.823 | 38.317 | 7544.943 | 7750.151 | 3148.088 | 4602.063 |
| 131 | 203.851 | 57.883 | 8.819 | 1.505 | 45.722 | 11620.630 | 12271.57 | 4984.675 | 7286.895 |
| 205 | 171.784 | 42.867 | 8.170 | 0.584 | 44.885 | 12359.551 | 11781.39 | 4785.563 | 6995.822 |
| 51 | 78.476 | 60.745 | 9.439 | 1.320 | 36.152 | 7370.700 | 7215.381 | 2930.866 | 4284.515 |
| 52 | 82.163 | 64.956 | 9.576 | 1.656 | 39.972 | 8256.199 | 7904.086 | 3210.616 | 4693.470 |
| **SUM** | | | | | | | **97318.44** | **39530.46** | **57787.98** |

to generate output in form of a computed volume of sediment loss-in-transit as a function of the normalised gully sectional sediment loss and dam's sediment accumulation. Our investigations showed that the ANFIS model could estimate sediment deposited in the dam effectively while, at the same time, it was able to determine the volume of sediment loss-in-transit using the established mathematical equation. The best ANN model with the least error and the most accurate predictive result was selected and presented. However, we made some assumptions. For example, we assume no silt (sediment) escapes from the dam by any means, (that is, the dam traps all the sediment behind it). The combined volume of sediment exited from the two gullies was treated as stagnant to be able to arrive at a numerical value. The volume of sediment deposited in the dam is treated as being localized (i. e. confined); such that numerical values can be obtained for location-based sediment volume actualisation. For these reasons, sediment transport equations were not incorporated. Furthermore, rather than converting the estimated sediment volume to weight equivalent, we left it in meters cubed to save processing time and computational space.

### 4.1. Recommendations

According to our discoveries in this work, we recommend the following:

Due to the fast rate of siltation, there is an urgent need to dredge the dam.

At present, sediment impact has rendered the Ikpoba dam a failed infrastructure, hence we propose a holistic desilting or dredging for the rejuvenation of the dam to return it back to its original purpose of providing domestic water for the teeming population.

Gully remediation action should be prioritize and attracts necessary attention from relevant government agencies and decisionmakers to enhance a safe environment devoid of land degradation.

## Acknowledgements

The authors are grateful to Iterlen Industrial Services Ltd, Km 1 Effurun-DSC Express Road, Ugbolokposo, Delta State for the release of the Hi-Target echo-sounder and accessories, the Department of Geomatics, University of Benin, for the assistance with the Total Station equipment used for data collection, the Department of Civil Engineering for allowing the laboratory to be used for soil analysis. The authors are also grateful to the Federal Government of Nigeria for providing part of the funding for this research through the tertiary education trust fund (TETFUND) initiative with grant No: REG/SSA/P.15799/83 (2018 intervention).

## References

[1] S. Chakraverty & S. Mall, "Artificial Neural Networks for Engineers and ScientistsSolving Ordinary Differential Equations", CRC Press **168** (2017) 80.
[2] S. Akram & R. Hossien, "Improving one-dimensional pollution dispersion modeling in rivers using ANFIS and ANN-based GA optimized models", *Environmental Science and Pollution Research* (2018).
[3] V. Umarania, A. Juliana & J. Deepa, "Sentiment Analysis using various Machine Learning and Deep Learning Techniques", J. Nig. Soc. Phys. Sci. **3** (2021) 308.
[4] C. I. Udeze, I. E. Eteng & A. E. Ibor, "Application of Machine Learning and Resampling Techniques to Credit Card Fraud Detection" J. Nig. Soc. Phys. Sci. **4** (2022) 769.
[5] B. N. Hikona, G. G. Yebpellaa, L. Jafiyab & S. Ayuba, "Preliminary Investigation of Microplastic as a Vector for HeavyMetals in Bye-ma Salt Mine, Wukari, Nigeria", J. Nig. Soc. Phys. Sci. **3** (2021) 259.
[6] G. O. Aigbadon, A. Ocheli, & E. O. Akudo, "Geotechnical evaluation of gully erosion and landslides materials and their impact in Iguosa and its environs, southern Nigeria", Environ Syst Res **10** (2021) 36.
[7] J. C. Egbueri, O. Igwe & C. O. Unigwe, "Gully slope distribution characteristics and stability analysis for soil erosion risk ranking in parts of southeastern Nigeria: a case study", Environ Earth Sci **80** (2021) 292.
[8] J. O. Ehiorobo & O. C. Izinyon, "Monitoring Gully Formation and Development for Effective Remediation and Control", TS09I - Engineering Surveying, 5919. FIG Working Week 2012. Knowing to manage the territory, protect the environment, evaluate the cultural heritage Rome, Italy (2012) 6.
[9] J. O. Ehiorobo, & O. C. Izinyon, "Monitoring of Soil Loss from Erosion Using Geoinformatics and Geotechnical Engineering Methods". (2011). Retrieved June 10, 2021, from https://www.fig.net/resources/proceedings/2011.
[10] O. Igwe, U. I. John, O. Solomon & O. Obinna., "GIS-based gully erosion susceptibility modeling, adapting bivariate statistical method and AHP approach in Gombe town and environs Northeast Nigeria", Geoenvironmental Disasters **7** (2020) 32.
[11] S. E. Okonofua & N. O. Uwadia, "Evaluating Factors Responsible for Gully Development at the University of Benin. Scholarlink Research Institute Journals", Journal of Emerging Trends in Engineering and Applied Sciences (JETEAS) **4** (2013) 5.
[12] S. Dahiru, "Nigeria Erosion and Watershed Management Project", (NEWMAP). (2020). Retrieved July 20, 2021, from https://newmap.gov.ng/index.php.
[13] World Bank, "Nigeria Erosion and Watershed Management Project (NEWMAP) Additional Financing" (2017). https://documents1.worldbank.org/curated/en/193161525194153230. Deposited July 10, 2022.
[14] N. Q. Sultan, E. Isa & R. M. Hossien, "Optimizing ANFIS for sediment transport in open channels using different evolutionary algorithms", Journal of Applied Research in Water and Wastewater **4** (2017) 1.
[15] X. Zhang, J. Fan, Q. Liu & D. Xiong, "The contribution of gully erosion to total sediment production in a small watershed in Southwest China", Physical Geography **39** (2018) 3.
[16] Y. Guan, S. Yang, C. Zhao, H. Lou, K. Chen, C. Zhang & B. Wu, "Monitoring long-term gully erosion and topographic thresholds in the marginal zone of the Chinese Loess Plateau", Soil and Tillage Research **205** (2021) 104800.
[17] I. Ionita, M. A. Fullen, W. Zgłobicki & J. Poesen, "Gully erosion as a natural and human-induced hazard", Nat Hazards **79** (2015) 1.
[18] C. Jiang, W. Fan, N. Yu & E. Liu, "Spatial modeling of gully head erosion on the Loess Plateau using a certainty factor and random forest model", Science of the Total Environment **783** (2021).
[19] I. Marzolff, J. Poeen & J. B. Ries, "Short to medium-term gully development: human activity and gully erosion variability in selected Spanish gully catchments", Landform Anal **17** (2011) 111.
[20] P. K. Shit, G. Bhunia & R. Maiti, "Morphology and development of selected Badlands in South Bengal (India)", Indian Journal of Geography and Environment **13** (2014) 161.
[21] G. Chen, "A simple way to deal with multicollinearity", Journal of Applied Statistics **39** (2012) 9.
[22] J. Poesen, J. Nachtergaele, G. Verstraeten & C. Valentin, "Gully erosion and environmental change: Importance and research needs", Catena **50** (2003) 91.
[23] A. Majhi, J. Nyssen & A. Verdoodt, "What is the best technique to estimate topographic thresholds of gully erosion? Insights from a case study on the permanent gullies of Rarh plain, India", Geomorphology **375** (2021) 107547.
[24] J. S. R. Jang, "ANFIS: adaptive-network-based fuzzy inference system", IEEE Trans. Syst. Man Cybern. **23** (1993) 665.
[25] J. S. R. Jang, "Input selection for ANFIS learning" In Proceedings of the Fifth IEEE International Conference on Fuzzy Systems (1996) 1493.
[26] J. S. R. Jang & E. Mizutani, "Levenberg–Marquardt method for ANFIS learning", In Fuzzy Information Processing Society, Biennial Conference of the North American (1996) 87.
[27] D. K. Ghosea, S. S. Pandab & P. C. Swainc, "Prediction and optimization of runoff via ANFIS and GA", Alexandria Engineering Journal **52** (2013) 2.
[28] T. Gokmen, O. Serhan & P. S. Vijay, "Fuzzy logic algorithm for runoff-induced sediment transport from bare soil surfaces", Advances in Water Resources **26** (2003) 1249.
[29] A. B. Dariane & S. H. Azimi, "Forecasting streamflow by combination of genetic input selection algorithm and wavelet transform using ANFIS model", Hydrolog. Sci. J. **61** (2016) 585.
[30] A. Mustafa, "Evaluation of different types of artificial intelligence methods to model the suspended sediment load in Tigris River", MATEC Web of Conferences **162** (2018) 2.
[31] H. M. Azamathulla & A. A. Ghani, "ANFIS-based approach for predicting the scour depth at culvert outlets", Journal of Pipeline Systems Engineering and Practice **2** (2011).
[32] H. M. Azamathulla, A. A. Ghani & S. Y., Fei, "ANFIS-based approach for predicting sediment transport in clean sewer", Applied soft computing **12** (2012) 3.
[33] H. M. Azamathulla, K C. Chun, A. A. Ghani, A. Junaidah, N. A., Zakaria & Z. A. Hasan, "An ANFIS-based approach for predicting the bed load for moderately sized rivers", Journal of Hydro-environment Research **3** (2009) 35.
[34] C. I. Ikhile, "Geomorphology and Hydrology of the Benin Region, Edo State, Nigeria", International Journal of Geosciences **7** (2016).
[35] C. N. Akujieze, "Effects of Anthropogenic Activities (Sand Quarrying and Waste Disposal) on Urban Groundwater System and Aquifer Vulnerability Assessment in Benin City, Edo State, Nigeria". PhD Thesis, University of Benin, Benin City, Nigeria (2004).
[36] P. Hjorth & L. Bengtsson, "Large Dams, Statistics and Critical Review". In: Bengtsson L., Herschy R.W., Fairbridge R.W. (eds) Encyclopedia of Lakes and Reservoirs, Encyclopedia of Earth Sciences Series, Springer, Dordrecht (2012).
[37] C. N. Ezugwu, B. U. Anyata & E. O. Ekenta, "Estimation of The Life of Ikpoba River Reservoir", International Journal of Engineering Research & Technology (IJERT) **2** (2013) 8.
[38] Edo State Urban Water Board, Construction information of Ikpoba Dam Archive (2007).

[39] S. O. Oladosu, L. M. Ojigi, V. E. Aturuocha, C. O. Anekwe & R. Tanko, "An investigative study on the volume of sediment accumulation in Tagwai dam reservoir using bathymetric and geostatistical analysis techniques", SN Applied Sciences **1** (2019) 492.
[40] International Hydrographic Organization (IHO) Standards for Hydrographic Surveys 6th Edition IHO Publication (2020) 44.
[41] B. Selma, S. Chouraqui & H. Abouaïssa, "Optimization of ANFIS controllers using improved ant colony to control an UAV trajectory tracking task", SN Appl. Sci. **2** (2020) 878.
[42] M. Sugeno, T. Kang & G. Kang, "Structure Identification of Fuzzy Model. Fuzzy Sets and Systems", 28 (1988) 9.
[43] T. Takagi & M. Sugeno, "Fuzzy Identification of Systems and Its Application to Modeling and Control", IEEE Transactions on Systems, Man, and Cybernetics, SMC-15 (1985).
[44] A. Tarno, Rusgiyono & Sugito, "Adaptive Neuro Fuzzy Inference System (ANFIS) approach for modeling paddy production data in Central Java", IOP Conf. Series: Journal of Physics: Conf. Series **1217** (2019) 012083.
[45] N. A. Adnan, H. Maizah & R. A. Adnan, "Comparative study on some methods for handling multicollinearity problems", Mathematika **22** (2006) 2.
[46] M. Kutner, C. J. Nacctsheim & J. Neter, "Applied Linear Regression Model". *Technometrics* **26** (2004) 4.
[47] D. W. Marquardt, "Generalized inverses, ridge regression, biased linear estimation, and nonlinear estimation", *Technometrics* **12** (1970) 59.
[48] D. O'brien & P. S. Scott, "Correlation and Regression", in Approaches to Quantitative Research-A guide for Dissertation Students, Ed, Chen, H, Oak Tree Press (2012).
[49] R. M. O'brien, "A Caution Regarding Rule of Thumb for Variance Inflation Factor", Qual Quant. **41** (2007) 673.